

Exploring Temporal Granularity in Self-Supervised Video Representation Learning

Rui Qian^{1,2} Yeqing Li¹ Liangzhe Yuan¹ Boqing Gong¹ Ting Liu¹
Matthew Brown¹ Serge Belongie³ Ming-Hsuan Yang¹ Hartwig Adam¹ Yin Cui¹
¹Google Research ²Cornell University ³University of Copenhagen

Abstract

This work presents a self-supervised learning framework named **TeG** to explore **Temporal Granularity** in learning video representations. In **TeG**, we sample a long clip from a video and a short clip that lies inside the long clip. We then extract their dense temporal embeddings. The training objective consists of two parts: a fine-grained temporal learning objective to maximize the similarity between corresponding temporal embeddings in the short clip and the long clip, and a persistent temporal learning objective to pull together global embeddings of the two clips. Our study reveals the impact of temporal granularity with three major findings. 1) Different video tasks may require features of different temporal granularities. 2) Intriguingly, some tasks that are widely considered to require temporal awareness can actually be well addressed by temporally persistent features. 3) The flexibility of **TeG** gives rise to state-of-the-art results on 8 video benchmarks, outperforming supervised pre-training in most cases.

1. Introduction

Learning visual representations from abundantly available unlabeled videos is of crucial importance in computer vision, as the extra time dimension in videos enriches their content while significantly increasing the cost of manual annotation. Thanks to the recent breakthroughs in image self-supervised learning [9, 13, 30, 34], a series of more recent works extended similar ideas to videos [20, 57, 58].

The success of recent video self-supervised learning methods largely depends on a seemingly counter-intuitive objective: enforcing temporal persistency across an entire video. More specifically, Qian *et al.* [57] randomly sample two clips from a video as the positive pair to maximize their feature similarity; Recasens *et al.* [58] require the feature of a sampled clip to be close to the feature of the whole video in different modalities; Feichtenhofer *et al.* [20] pull together features from multiple clips within a video and observe that encouraging long temporal persistency can be effective even if the timespan is up to 60 seconds.

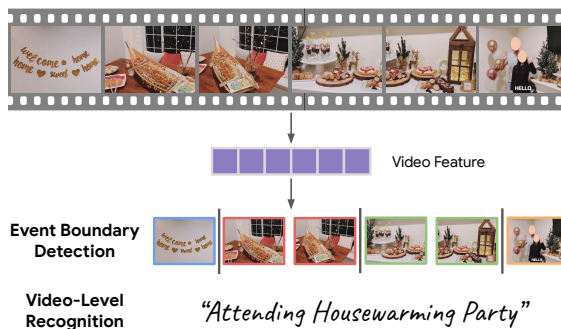


Figure 1. Illustration of tasks requiring different temporal granularities on the same short video. Event boundary detection requires temporally fine-grained features within the video to achieve good performance, while in the case of video-level recognition, temporally persistent features are preferred.

Despite the strong performance on commonly used video benchmarks (e.g., action recognition [39, 42, 70]), we find that features learned with such an objective do not perform well on more challenging video tasks proposed recently that require fine-grained temporal predictions [61, 65]. This poses an interesting question: how can we develop a video self-supervised learning framework that accounts for both fine-grained and persistent temporal information?

We answer this question by rethinking video representation learning from the perspective of temporal granularity. The concept of temporal granularity has been studied in speech recognition [23] and time series analysis [5, 15], but is rather under-explored in the recent video representation learning research. We find that different video tasks may require features of different temporal granularities. In Figure 1, the event boundary detection calls for temporally fine-grained features so that the model is aware of the temporal content shifts. In contrast, video-level recognition requires the model to robustly predict the target label based on some sampled clips from the video; therefore, temporally persistent/coarse-grained features are more desirable.

The temporal dynamics of videos naturally provides a rich source of supervision for learning features with varying temporal granularities. As illustrated in Figure 2, we propose **TeG**, a framework to explore **Temporal Granularity**

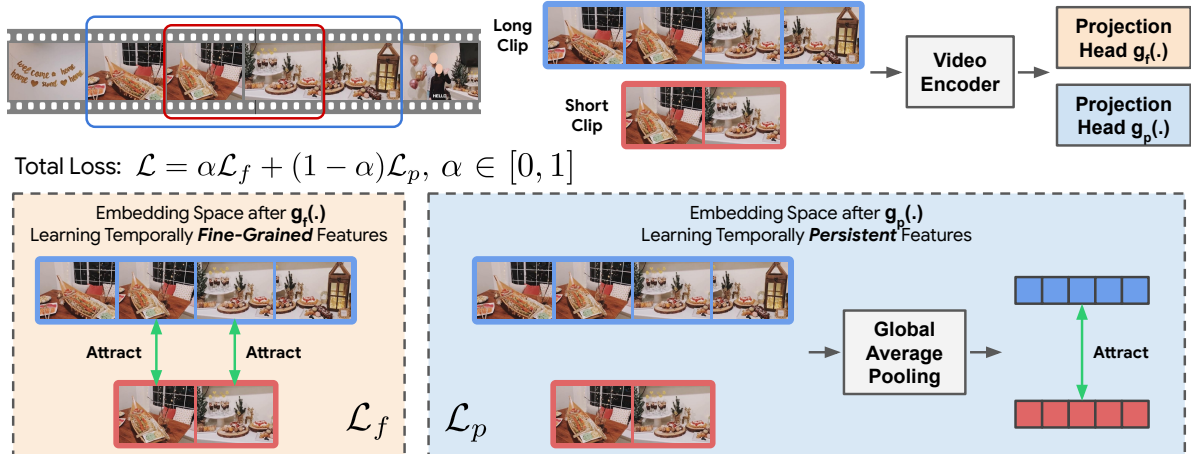


Figure 2. Overview of our proposed TeG framework. We randomly sample a long clip from a given video and a short clip that lies inside the long clip. We then feed two clips into a video encoder without applying the final temporal average pooling. Two projection heads are applied to project features into separate embedding spaces, one for learning temporally fine-grained features and the other for learning temporally persistent features. For simplicity, spatial data augmentations and negative pairs from different videos are not illustrated.

via the combination of fine-grained and persistent temporal learning. In TeG, we randomly sample a long clip from a video and a short clip that lies inside the time duration of the long clip. We then feed them into a video encoder without applying the final temporal average pooling. The resultant features are projected into two separate embedding spaces with different contrastive learning objectives.

In the fine-grained temporal learning space, for each clip, we split the projected features along the temporal dimension into a list of temporal embeddings, each represents the feature of a short time duration. Our sampling strategy guarantees that each temporal embedding in the short clip has a corresponding temporal embedding in the long clip at approximately the same start and end time. We apply a dense contrastive objective to maximize the similarity between corresponding temporal embeddings, which explicitly encourages temporal embeddings to be discriminative within a clip, making the learned features temporally fine-grained.

In the temporally persistent feature learning space, we directly apply a global average pooling to generate the global embedding for both the short clip and the long clip. The training objective here encourages global temporal persistency by pulling together two embeddings, similarly to what has been used in existing frameworks [20, 57, 58]. Our sampling strategy makes sure the global embedding from the long clip contains rich spatiotemporal context to avoid the model overly fitting to learning local features only.

TeG optimizes both objectives and offers a flexible solution to learning features of different temporal granularities by adjusting the loss weight between the two objectives.

To understand the impact of the temporal granularity, we leverage two recently proposed datasets for understanding events in short videos to challenge self-supervised

video representation learning: VidSitu event classification [61] and Kinetics-GEED (generic event boundary detection) [65]. We conduct comprehensive experiments on the new benchmarks together with other commonly used video benchmarks. We next summarize our main findings.

First, **different video tasks may require features of different temporal granularities**. For example, learning temporally fine-grained features improves the performance on VidSitu by 2.8% and Kinetics-GEED by 1.5%, but hurts Kinetics linear evaluation by 2.8%. See Tables 1, 2 and 3.

However, intriguingly, **temporally persistent features achieve strong performance on some video tasks that are widely considered requiring temporal awareness**. Specifically, we achieve 61.4% on Something-Something-v2 (SSv2) and 83.6% on Diving48 with only the temporal persistency objective in TeG. Our performance on Diving48 largely outperforms the supervised pre-training counterpart by 6.0%. Surprisingly, adding the fine-grained temporal learning objective yields a performance drop of 0.9% on SSv2 and 2.1% on Diving48. See Tables 4 and 5.

Finally, video representations learned with TeG advance the **state-of-the-art on a wide range of video tasks**. In addition to the above mentioned results, TeG obtains a strong performance of 67.8% on Kinetics linear evaluation. Fine-tuning the learned features on Kinetics yields 28.7 mAP on AVA-Kinetics, 94.1% on UCF, and 71.9% on HMDB. Our result on AVA-Kinetics significantly outperforms the supervised pre-training counterpart by 8.9 mAP. See Tables 3, 7 and 6. Other than classic video benchmarks, we achieve 31.1% accuracy on VidSitu, which is on par with the supervised pre-training. On Kinetics-GEED, TeG obtains 71.4% F1 score, outperforming a strong supervised pre-training method by a large margin of 8.9%. See Tables 1 and 2.

2. Related Work

Unsupervised video representation learning. The temporal dimension of video has been densely explored. In an early work, Srivastava *et al.* [71] propose to predict the future based on frame features. More recent work learn from raw videos by predicting motion and appearance statistics [76], speed [6, 77] and encodings [31, 32, 52]. Aside from future prediction, it is common to learn from pretext tasks like sorting frames or video clips [22, 40, 44, 79] and rotation [38]. Recently, contrastive learning based methods [20, 57, 58, 69] significantly reduce the gap with supervised learning by pulling together features of clips from the same video. Furthermore, videos containing multi-modal signals make it possible to learn from cross-modality self-supervision, *e.g.* geometric cues [24], speech or language [53, 72, 73], audio [3, 4, 41, 55], optical flow [33], or combinations of multiple modalities [1, 2, 58] and tasks [56]. Different from existing work, we introduce temporally fine-grained features into the video contrastive learning framework and study its impact on various downstream tasks.

Fine-grained temporal video understanding. We first discuss two representative tasks: temporal localization and segmentation. Commonly used temporal localization benchmarks (*e.g.*, ActivityNet [8], THUMOS [37], HACS [83]) are constructed based on specified action classes. As a result, most temporal localization methods [49–51, 66, 67, 84] contain a temporal proposal module to simply treat video segments that do not belong to pre-defined classes as the background. Temporal segmentation methods [18, 43, 60] typically divide a video into segments of actions, or sub-actions [62, 63]. But still, those methods can only predict boundaries of pre-defined classes, not generic boundaries. On the other hand, studies in cognitive science [74] show that humans naturally segment videos into meaningful temporal chunks of events, without pre-defined categories. Inspired by this, we choose the recently proposed Kinetics-GEBD [65] dataset to verify whether TeG is able to learn temporally fine-grained features that can be used for generic event boundary detection. We also benchmark our method on AVA-Kinetics [45], a classic spatiotemporal action localization dataset. In addition to videos containing human actions, movies could also provide rich content for fine-grained temporal video understanding. However, temporal movie understanding methods [12, 36, 54] typically focus on shots, which are defined by sharp transitions due to video editing and can be accurately localized using low-level visual cues [68]. To better benchmark our method in complex movie scenes, we adopt the recently proposed VidSitu [61] dataset. In VidSitu, each short video is temporally annotated with 5 events. Transitions between events are usually natural and continuous, and thus cannot be detected by low-level visual cues.

3. Method

Our proposed framework is illustrated in Figure 2. We next introduce each component in detail.

Temporal sampling. Given a video of N frames, $V = \{v_1, v_2, \dots, v_N\}$, previous works [20, 57] typically sample two short clips with the same length independently from V aiming at learning temporally persistent features. However, this common strategy is not suitable for learning temporally fine-grained features since it enforces non-overlapped clips to have similar features. Sampling two clips that have some overlaps would partially avoid this issue, but it sacrifices diversity in spatiotemporal context, resulting in inferior representations. Hence, we propose a long-short sampling strategy, where we first sample a long clip l randomly from the whole video, and then we sample a short clip s from the whole video inside the time duration of the long clip. The long clip provides rich spatiotemporal context, and the short clip in it ensures the existence of corresponding embeddings between the two clips. The ablation on sampling strategy is in Table 8.

We note that some very recent works [58, 75] also propose an asymmetric sampling strategy. Our method differs from them in the following key aspects: 1) Motivation: we propose this design to find corresponding embeddings and preserve rich spatiotemporal context at the same time, while Recasens *et al.* [58] aim at accommodating different modalities, and Wang *et al.* [75] focus on pre-training for video transformers. 2) Objective: we use this design to learn temporally fine-grained features. In contrast, their works [58, 75] still emphasize the invariance across the whole video. 3) Implementation: based on our motivation and objective, we require the short clip to fall inside the long clip, while they [58, 75] perform independent sampling which is similar to other video self-supervised learning methods using symmetric sampling [20, 57]. Finally, we conduct dense contrastive learning between corresponding embeddings, which is fundamentally different from their work [58, 75].

Spatial data augmentation. After obtaining the short clip s and long clip l , we adopt the common practice in recent video contrastive learning [2, 3, 57] and apply a series of spatial data augmentations including random resizing and cropping, color jittering, and Gaussian blurring. The parameters of the spatial augmentations follow Qian *et al.* [57].

Video encoder. We adopt the 3D-ResNet-50 (R3D-50) backbone architecture used in [57]. We remove the final *temporal* average pooling and only keep the global *spatial* average pooling since we are primarily interested in exploring *temporal* granularities. We notate the modified encoder as $f(\cdot)$. We apply two projection heads: $g_p(\cdot)$ for persistent temporal learning and $g_f(\cdot)$ for fine-grained temporal learning. They project representations into separate

embedding spaces with different contrastive objectives. In the persistent learning space, we obtain embedding z_p^s from the short clip input s and z_p^l from the long clip input l by $\{z_p^s, z_p^l\} = \{g_p(f(s)), g_p(f(l))\}$; in the fine-grained learning space, we have $\{z_f^s, z_f^l\} = \{g_f(f(s)), g_f(f(l))\}$.

Our approach maintains a simple form of video contrastive learning where we do not use separate encoders for different clips [58], nor do we use a momentum encoder [20], predictor head [20, 75] and symmetric losses [58]. Extensive experiments in Section 5 demonstrate the effectiveness of this simple design.

Temporal aggregation. For temporally persistent learning, as a common practice [20, 57], we directly apply a global average pooling along the temporal dimension to get a single vector representing the whole clip, resulting in $z_p^s, z_p^l \in \mathbb{R}^{1 \times c}$, where c is the number of output channels from the projection head. For temporally fine-grained learning, we design a configurable local aggregation strategy to optionally aggregate consecutive local temporal embeddings to reduce training complexity. We denote the number of frames in short clip s and long clip l as T_s and T_l , respectively. Our aggregation strategy performs average pooling on every consecutive $\frac{T_s}{n}$ frames in the short clip and every consecutive $\frac{T_l}{m}$ frames in the long clip, resulting in aggregated outputs of $z_f^s \in \mathbb{R}^{n \times c}$ and $z_f^l \in \mathbb{R}^{m \times c}$. When $n = 1$ and $m = 1$, it reduces to temporal persistent learning. When $n = T_s$ and $m = T_l$, it conducts dense temporal contrastive learning on frame-level embeddings. Figure 4 ablates the effect of different choices of n and m . We further use $z_f^s[i]$ to index the i -th dimension of z_f^s and $z_f^l[j]$ to index the j -th dimension of z_f^l , where $1 \leq i \leq n$ and $1 \leq j \leq m$.

Fine-grained temporal learning. We aim to obtain temporally fine-grained features by maximizing the feature similarity between corresponding embeddings of the short and the long clip. The corresponding embeddings should be close in time and we rely on the frame index to find them. Since we conduct temporal aggregation on a few consecutive frames, we define the index of a certain embedding $z_f^s[i]$ after aggregation as the average frame index of all aggregated frames, notated as $I(z_f^s[i])$. We find $z_f^s[i]$'s corresponding embedding $z_f^l[j]$ in the long clip by:

$$j = \arg \min_j |I(z_f^s[i]) - I(z_f^l[j])|. \quad (1)$$

$(z_f^s[i], z_f^l[j])$ has the closest temporal distance and it is considered as the positive pair. The fine-grained temporal learning loss can be written as:

$$\mathcal{L}_f = -\frac{1}{n} \sum_{i=1}^n \log \frac{\exp(z_f^s[i] \cdot z_f^l[j]/\tau)}{\exp(z_f^s[i] \cdot z_f^l[j]/\tau) + \sum_{k_f^-} \exp(z_f^s[i] \cdot k_f^-/\tau)}, \quad (2)$$

where k_f^- represents all dense embeddings of long clips from other videos after temporal aggregation in the fine-grained temporal learning space and τ is the temperature.

Persistent temporal learning. Recall that we have embeddings $z_p^s, z_p^l \in \mathbb{R}^{1 \times c}$ in the temporally persistent learning space. (z_p^s, z_p^l) is considered as the positive pair and (z_p^s, k_p^-) are considered as negative pairs, where k_p^- represents all global embeddings from long clips of other videos in the persistent temporal learning space. The persistent temporal learning loss can be written as:

$$\mathcal{L}_p = -\log \frac{\exp(z_p^s \cdot z_p^l/\tau)}{\exp(z_p^s \cdot z_p^l/\tau) + \sum_{k_p^-} \exp(z_p^s \cdot k_p^-/\tau)}. \quad (3)$$

\mathcal{L}_p adopts the same temperature τ with \mathcal{L}_f for simplicity.

Total loss. The total loss is a weighted sum of the fine-grained and persistent temporal learning loss:

$$\mathcal{L} = \alpha \mathcal{L}_f + (1 - \alpha) \mathcal{L}_p, \quad (4)$$

where the weight $\alpha \in [0, 1]$ is used to control the temporal granularity of the learned features. When α is close to 0, we intend to learn temporally persistent features with only \mathcal{L}_p in the loss. With the increasing of α , more temporally fine-grained features will be obtained. An ablation regarding the effect of α on two datasets is presented in Figure 3.

4. Evaluation

To evaluate our proposed framework, we leverage two recently proposed datasets: VidSitu [61] for event classification and Kinetics-GEBD [65] for generic event boundary detection. Additionally, we also evaluate on 6 commonly used datasets, including Kinetics via linear probing and various downstream tasks via fine-tuning. See Section 5 for more details. We next describe how we evaluate our method on these 2 new datasets.

Event classification. VidSitu [61] is a large-scale movie dataset focusing on understanding the relationship of events in short videos. Each video in VidSitu is 10-second long and divided into 5 consecutive and non-overlapping events. Each event is annotated with a verb to describe the most salient action taking place inside it. The temporal duration of the events is determined by human perception to avoid including multiple events. The baseline provided by the original authors is to first cut the video into 5 events according to the annotated boundaries and then perform classification for each event. In our case, we directly apply our method on raw videos in VidSitu without using any labels in pre-training. An interesting property of this dataset is that the transition between events is usually natural and continuous, and cannot be easily detected by an off-the-shelf shot detector [68]. Thus we consider VidSitu a good benchmark to

evaluate whether our method can learn more fine-grained temporal features than current state-of-the-art video-level persistent learning methods [57]. We adopt linear probing in the evaluation, where we use their event labels to train a linear classifier on top the frozen backbone to quantify the performance of the learned representations.

Generic event boundary detection. Kinetics-GEBD [65] annotates Kinetics-400 [39] videos with fine-grained event boundaries based on human perception. The boundaries are in the format of timestamps and a detection is considered as correct when its temporal distance with a ground truth is smaller than 5% of the total video length. We use a 1D sliding window detection method to detect event boundaries, following the spirit of classic object detection methods like HOG [16] and DPM [21]. We first pre-train our backbone without using any annotations. We then add a binary linear classifier on top of the pre-trained backbone to predict whether a clip contains a boundary or not. Similar to object detection [26,59], we fine-tune the model end-to-end to verify the performance of our learned features.

5. Experiments

We first introduce general implementation details, followed by task-specific settings and experimental results.

5.1. Implementation Details

We use SGD with the momentum of 0.9 as our optimizer. During the self-supervised pre-training, we follow [57] to train models with 1024 batch size and 0.32 learning rate, using linear warm up in the first 5 epochs [28] followed by half-period cosine decay [35]. The temperature τ in loss function is set to 0.156 for pre-training on Kinetics, and 0.1 for all other datasets. We adopt two representative settings in our method: 1) $\alpha = 0.0$ for persistent temporal learning only and we call this method **TeG-PS**, where PS represents “persistent”. 2) $\alpha = 0.9$, in which the fine-grained temporal learning loss is the dominant loss and we denote this method as **TeG-FG**, where FG represents “fine-grained”. Our code and models will be made available to the public.

5.2. Event Classification

We conduct experiments on VidSitu [61], which contains 23.6k training and 1.3k validation videos from 1560 verb classes. Each video is exactly 10-second long and is divided into 5 event clips. Each event clip in the validation set receives 10 annotations to respect the flexibility of describing an event with multiple similar verbs. During pre-training, we sample a 32-frame long clip with a stride of 4 and a 16-frame short clip with a stride of 2. Temporal aggregation parameters are set as $m = 4$ and $n = 1$ (ablation study in Figure 4). We pre-train our model from scratch for 200 epochs on unlabeled raw videos. During the linear evaluation, we

train a linear classifier with an initial learning rate of 4.0 for 100 epochs. To deal with multiple human annotations in the validation set, we follow the practice from the original authors [61] by only considering the set of classes that appear at least twice within the 10 annotations. A prediction would be considered as correct if it matches any class in the set. Additional details can be found in Appendix A.1.

We show TeG’s performance on VidSitu in Table 1. The supervised methods directly train models from scratch on the training set, using labels for each event clip cut from raw videos. The unsupervised methods perform pre-training on raw videos from scratch without using any labels and then conduct linear evaluation. We adopt CVRL [57] as an important baseline since it is a representative method that enforces temporal persistency across the whole video. TeG-PS achieves similar performance with CVRL while TeG-FG equipped with temporally fine-grained pre-training improves the performance by 2.8%. Furthermore, the performance TeG-FG is on par with supervised methods using I3D as the backbone. This result provides a solid evidence that temporal persistent learning is not the optimal solution on this event classification benchmark.

method		backbone	acc.
		I3D	31.2
Supervised	Train from scratch [61]	I3D + NL	30.2
		R3D-50 + NL	33.1
		SlowFast + NL	32.6
		CVRL [57]	28.3
Unsupervised	TeG-PS	R3D-50	28.3
	TeG-FG	R3D-50	31.1

Table 1. **Event classification on Vidsitu.** TeG-FG with fine-grained temporal learning outperforms persistent temporal learning and is on par with supervised methods.

5.3. Generic Event Boundary Detection

We perform experiments on Kinetics-GEBD [65], which contains 20k out of 240k Kinetics-400 [39] training videos and all 20k validation videos, each annotated with 5 sets of event boundaries. We sample a 16-frame long clip and a 8-frame short clip, both with a stride of 2. Temporal aggregation parameters are set as $m = 2$ and $n = 1$. We pre-train our model from scratch for 200 epochs and then fine-tune the model with the annotated boundaries for 30 epochs. The temporal sliding window is set with a duration of 1.28s and a stride of 0.12s to go through all videos to generate all clips. The clips are considered as positive when the timestamp of the clip’s center is within 0.15s of the annotated boundaries, following the original authors [65]. This results in 0.2M positive and 1.2M negative clips in total. Balanced sampling is applied for each training batch to avoid the model overly focusing on negative examples. For evaluation, we compare our prediction with all annotations in the

same video and select the annotation with the highest F1 score as the ground-truth, which is the standard practice in the official evaluation code provided the authors [65]. Additional details can be found in Appendix A.2.

TeG’s performance on Kinetics-GEBD is presented in Table 2, where we report results using their strictest temporal threshold of 0.05 to emphasize on the importance of precise boundary detection. We first briefly introduce a few representative methods for this benchmark. SceneDet [11] is a widely-used library for detecting shot changes. BMN [49] is a state-of-the-art method for action proposal generation and here the start and end of each proposal are considered as event boundaries. The dataset creators [65] also develop an improved version of BMN called BMN-SE. TCN [43] is a classic action boundary detection method. PC [65] is the state-of-the-art method on this benchmark provided by performing pairwise classification around event boundaries. We group these methods by the external data they pre-train on and whether they fine-tune or keep the backbone frozen. From results in Table 2, finetuning methods clearly achieve much better performances. Compared to PC which relies on ImageNet supervised pre-training, CVRL [57] and TeG can directly pre-train on the training videos without using labels and external data for supervision. We draw a similar observation with event classification that TeG-FG with temporally fine-grained learning outperforms methods enforcing temporal persistency like CVRL and TeG-PS.

method	external data	finetuning	F1
BMN [49]	IN + THUMOS	✗	18.6
SceneDet [11]	-	✗	27.5
PA [65]	IN	✗	39.6
BMN-SE [49]	IN + THUMOS	✗	49.1
TCN [43]	IN	✗	58.8
PC [65]	IN	✓	62.5
CVRL [57]	-	✓	69.1
TeG-PS	-	✓	69.9
TeG-FG	-	✓	71.4

Table 2. **Event boundary detection on Kinetics-GEBD.** IN represents ImageNet supervised pre-training and THUMOS means additional supervised training on THUMOS [37]. TeG-FG with fine-grained temporal learning shows better performance than persistent temporal learning methods TeG-PS and CVRL. TeG-FG also surpass PC with ImageNet supervised pre-training by 8.9%.

5.4. Kinetics Linear Evaluation

We pre-train our model from scratch for 800 epochs on Kinetics-400 [39]. We use the same parameters with event classification: the long clip of 32-frame (4-stride), the short clip of 16-frame (2-stride) and the temporal aggregation of $m = 4, n = 1$. We perform linear evaluation which we consider as the most straightforward way to quantify the

method	backbone	pre-train data	acc.
VTHCL [81]	R3D-50	K400	37.8
SimCLR [57]	R3D-50	K400	46.8
VINCE [27]	R-50	K400	49.1
ImageNet [57]	R3D-50	IN	53.5
SeCo [82]	R-50	IN [†] + K400	61.9
ρ SwAV ($\rho=2$) [20]	R3D-50	K400	63.2
CVRL [57]	R3D-50	K400	66.1
ρ BYOL ($\rho=2$) [20]	R3D-50	K400	66.2
MCL [46]	R(2+1)D-50	IN [†] + K400	66.6
ρ MoCo ($\rho=2$) [20]	R3D-50	K400	67.4
TeG-FG	R3D-50	K400	65.0
TeG-PS	R3D-50	K400	67.8

Table 3. **Linear evaluation on Kinetics-400 action recognition.** For fair comparison, we quote results in [20] under the same setting with $\rho=2$ (sampling two clips from a video) and 800 epochs of pre-training. IN[†] denotes a MoCo-v2 [14] checkpoint pre-trained on ImageNet is used as the initialization of the backbone.

learned feature quality, following the same setting in [57]. As shown in Table 3, TeG-FG obtains 65.0% top-1 accuracy which trails behind some state-of-the-art methods such as CVRL [57] and ρ MoCo [20]. By contrast, TeG-PS achieves 67.8%, which is state-of-the-art on Kinetics linear evaluation without using multi-clip sampling [20] in pre-training. This verifies that temporal persistency is the key to obtain strong performance on Kinetics. We believe the performance of TeG-PS could be additionally boosted by multi-clip sampling as it further enhances temporal persistency.

5.5. Downstream Action Recognition

For the downstream action recognition task, we finetune the same pre-trained checkpoint from Kinetics linear evaluation on four benchmarks: Something-Something-v2 (SSv2) [29], Diving48 [47], UCF101 [70] and HMDB51 [42]. We attach a linear layer with a dropout rate of 0.5 after the backbone and train the model end-to-end for 50 epochs on all these benchmarks, with different learning rates of 3.0 for SSv2, 2.0 for Diving48, 0.64 for UCF and 0.32 for HMDB.

Something-Something-v2 and Diving48 are two representative datasets that are widely considered requiring temporal awareness and we first study the transfer performance on them. We find the two benchmarks in fact can be well addressed by solely learning temporally persistent features and bringing in temporally fine-grained features is detrimental. Concretely, as shown in Table 4, TeG-PS achieves 61.4% accuracy, surpassing TeG-FG as well as all other state-of-the-art unsupervised pre-training methods on SSv2. More surprisingly, TeG-PS, using a small R3D-50 backbone, is 1.9% better than TimeSformer and on par with SlowFast with supervised pre-training.

We observe similar trends from the results on Diving48

	method	pre-train data	acc.
	TimeSformer [7]	ImageNet	59.5
Sup. pre-train	SlowFast [19]	K400	61.7
	TimeSformer-L [7]	ImageNet	62.0
	TSM [48]	K400	63.3
Unsup. pre-train	ρ MoCo ($\rho=2$) [20]	K400	54.4
	ρ BYOL ($\rho=2$) [20]	K400	55.8
	CVRL [57]	K400	59.6
	TeG-FG	K400	60.5
	TeG-PS	K400	61.4

Table 4. **Action recognition on Something-Something-v2.** Despite the dataset is considered requiring more temporal awareness, TeG-PS outperforms TeG-FG, and is on par with strong supervised pre-training methods.

in Table 5, where the advantage of TeG-PS is further enhanced. TeG-PS achieves 83.6%, which is more than 2% better than TeG-FG and CVRL. Note that we adopt the updated annotations (Oct. 2020)¹ provided by the original author, where the mislabelled data are corrected. For fair comparison, all results we report here are conducted on the updated annotations. To our surprise, simply using unsupervised pre-training and a R3D-50 backbone, TeG-PS is able to obtain significantly better performance than state-of-the-art supervised pre-training methods using much stronger backbones, *e.g.* SlowFast [19], TimeSformer and TimeSformer-L [7].

	method	pre-train data	acc.
	I3D [10]	K400	48.3
Sup. pre-train	TSM [48]	ImageNet	51.1
	TSN [78]	ImageNet	52.5
	TimeSformer [7]	ImageNet	74.9
	SlowFast [19]	K400	77.6
	TimeSformer-L [7]	ImageNet	81.0
Unsup. pre-train	CVRL [57]	K400	80.9
	TeG-FG	K400	81.5
	TeG-PS	K400	83.6

Table 5. **Action recognition on Diving48.** TeG-PS sets a new record of 83.6% accuracy, outperforming all unsupervised and supervised pre-training methods.

We then report TeG’s performance on UCF101 and HMDB51 in Table 6, which are classic benchmarks for evaluating self-supervised video representation learning. On UCF, TeG-PS achieves state-of-the-art performance of 94.1% with fine-tuning and 91.1% with linear evaluation. On HMDB, TeG-PS achieves 71.9% with fine-tuning which surpasses CVRL by 4% and 64.2% with linear evaluation which is 5.9% better than CVRL.

¹<http://www.svcl.ucsd.edu/projects/resound/dataset.html>

method	pre-train data	UCF	HMDB
Fine-Tuning			
MotionPred [76]	K400	61.2	33.4
3D-RotNet [38]	K400	64.5	34.3
ST-Puzzle [40]	K400	65.8	33.7
ClipOrder [79]	K400	72.4	30.9
DPC [31]	K400	75.7	35.7
PacePred [77]	K400	77.1	36.6
MemDPC [32]	K400	78.1	41.2
SpeedNet [6]	K400	81.1	48.8
CoCLR [33]	K400	87.9	54.6
DynamoNet [17]	YT8M	88.1	59.9
SeCo [82]	IN [†] + K400	88.3	55.6
CVRL [57]	K400	92.9	67.9
ρ MoCo ($\rho=2$) [20]	K400	93.2	-
MCL [46]	IN [†] + K400	93.4	69.1
TeG-FG	K400	93.6	70.7
TeG-PS	K400	94.1	71.9
Linear Evaluation			
MemDPC [32]	K400	54.1	30.5
CoCLR [33]	K400	77.8	52.4
CVRL [57]	K400	89.8	58.3
TeG-FG	K400	88.9	60.7
TeG-PS	K400	91.1	64.2

Table 6. **Action recognition on UCF101 and HMDB51.** TeG-PS shows superior performance over other methods. IN[†] denotes a MoCo-v2 [14] checkpoint pre-trained on ImageNet is used as the initialization of the backbone.

5.6. Downstream Action Localization

AVA-Kinetics [45] provides an important spatiotemporal action localization benchmark for evaluating the learned video features. We use our pre-trained backbone to extract features from the given clip. Following the practice in recent work [25, 45], we use an action transformer head to capture the relationship between each person and the whole scene, and conduct training using ground truth boxes and evaluate on person detections provided by an off-the-shelf detector [85]. We fine-tune the whole network for 36 epochs with an initial learning rate of 0.01 and a batch size of 256.

The results are shown in Table 7, where TeG-PS achieves 28.7 mAP, outperforming supervised pre-training on Kinetics using the same R3D-50 backbone by a large margin of 8.9 mAP. TeG-PS also shows superior performance when compared with other state-of-the-art unsupervised pre-training methods like CVRL and VFS [80]. TeG-FG is 1.0 mAP lower than TeG-PS, indicating that learning temporally fine-grained feature is not helpful on this task.

6. Ablation Study

We conduct ablation studies on a few key parameters in our proposed method. We use linear evaluation on VidSitu event classification to justify the performance on temporally

	method	pre-train data	mAP
Sup.	R3D-50	K400	19.8
pre-train	I3D [10]	ImageNet	22.9
	CVRL [57]	K400	24.1
Unsup.	VFS [80]	K400	25.9
pre-train	TeG-FG	K400	27.7
	TeG-PS	K400	28.7

Table 7. **Spatiotemporal action localization on AVA-Kinetics.** TeG-PS outperforms its supervised pre-training counterpart by 8.9 mAP using the same R3D-50 backbone, as well as state-of-the-art unsupervised pre-training methods.

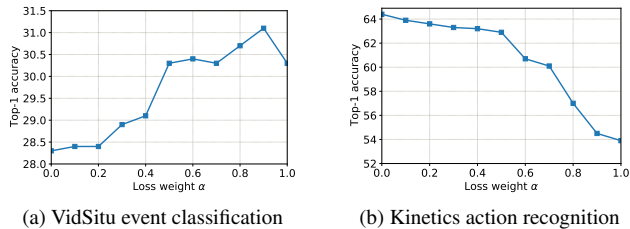


Figure 3. **Ablation on loss weight α .** VidSitu event classification and Kinetics action recognition require features of different granularities specified by α .

fine-grained task and linear evaluation on Kinetics to represent video-level classification task. All experiments are conducted with 200 epochs of pre-training.

Loss weight. Recall that in Equation 4, we propose to use a weight α to balance the learning of fine-grained and persistent loss. Intuitively, larger α would emphasize more on temporally fine-grained features and suppress the temporal persistency. We ablate the impact of α in Figure 3. On VidSitu (Figure 3a), we observe that larger α generally yields better performance as expected except a performance drop from when α increases from 0.9 to 1.0. This suggests that completely discarding the temporally persistent learning is not optimal. This is also the reason why we set α as 0.9 instead of 1.0 in TeG-FG. On Kinetics (Figure 3b), we see a consistent drop on the performance as α becomes larger. The reverse trend of performance further enhances our claim that different video tasks require features of different temporal granularities to achieve the best performance. Since we find bringing in temporally fine-grained features is harmful to Kinetics, we focus on VidSitu for the following ablation studies on parameters of temporally fine-grained learning. To further demonstrate the effect of loss weight on learned features, We visualize the feature similarity of TeG-PS and TeG-FG in Appendix B.

Sampling strategy. The proposed sampling strategy requires: 1) two clips to be asymmetric and 2) the short clip being contained in the long clip. We ablate on these two design choices in Table 8. When two clips are both short, random sampling is identical to CVRL [57] and contained

sampling loses the diversity in temporal context, thus resulting in poor performance. When two clips are asymmetric, random sampling still does not work well since the corresponding embeddings between the two clips are inaccurate in the cases that two clips do not have much overlap with each other.

clip \ sampling	Random	Contained
Short - Short	27.4	15.2
Long - Short	26.9	31.1

Table 8. **Ablation on sampling strategy.** The proposed sampling of a long clip and a containing short clip performs the best. Results are on VidSitu event classification.

Temporal aggregation. The temporal aggregation parameters m and n determine how dense we want our fine-grained learning to be. We try different combinations of m and n and present their performances in Figure 4. We choose $m = 4, n = 1$ as our default setting due to the simplicity and strong performance.

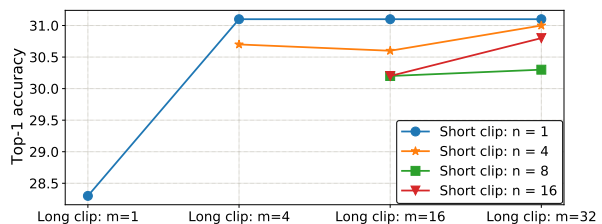


Figure 4. **Ablation on the choice of n and m in temporal aggregation.** Results are on VidSitu event classification.

7. Conclusions and Discussion

This work studies the impact of temporal granularity in self-supervised video representation learning. We propose a flexible framework, which we call TeG, to learn video features of specified temporal granularity and observe that different video tasks require features of different temporal granularities. This insight leads to state-of-the-art results on 8 video benchmarks. We hope our study can inspire researchers in advancing video self-supervised learning.

Limitations. As observed from the experimental results, we find temporally fine-grained feature performs better on tasks like event classification and boundary detection, while temporally persistent feature shows great advantage on video-level action recognition and spatiotemporal action localization. Manual effort is still needed to find the best recipe for different tasks. We hope our future work could extend TeG to learn a pyramid of representations with coarse to fine temporal granularities from unlabeled videos. Then the learned representations can be easily transferred to downstream tasks in a more adaptive way.

References

- [1] Hassan Akbari, Linagzhe Yuan, Rui Qian, Wei-Hong Chuang, Shih-Fu Chang, Yin Cui, and Boqing Gong. Vatt: Transformers for multimodal self-supervised learning from raw video, audio and text. In *NeurIPS*, 2021. 3
- [2] Jean-Baptiste Alayrac, Adrià Recasens, Rosalia Schneider, Relja Arandjelović, Jason Ramapuram, Jeffrey De Fauw, Lucas Smaira, Sander Dieleman, and Andrew Zisserman. Self-supervised multimodal versatile networks. In *NeurIPS*, 2020. 3
- [3] Humam Alwassel, Dhruv Mahajan, Lorenzo Torresani, Bernard Ghanem, and Du Tran. Self-supervised learning by cross-modal audio-video clustering. In *NeurIPS*, 2020. 3
- [4] Yuki M Asano, Mandela Patrick, Christian Rupprecht, and Andrea Vedaldi. Labelling unlabelled videos from scratch with multi-modal self-supervision. In *NeurIPS*, 2020. 3
- [5] Hamed Azami, Alberto Fernández, and Javier Escudero. Multivariate multiscale dispersion entropy of biomedical times series. *Entropy*, 2019. 1
- [6] Sagie Benaim, Ariel Ephrat, Oran Lang, Inbar Mosseri, William T Freeman, Michael Rubinstein, Michal Irani, and Tali Dekel. Speednet: Learning the speediness in videos. In *CVPR*, 2020. 3, 7
- [7] Gedas Bertasius, Heng Wang, and Lorenzo Torresani. Is space-time attention all you need for video understanding? In *ICML*, 2021. 7
- [8] Fabian Caba Heilbron, Victor Escorcia, Bernard Ghanem, and Juan Carlos Niebles. Activitynet: A large-scale video benchmark for human activity understanding. In *CVPR*, 2015. 3
- [9] Mathilde Caron, Ishan Misra, Julien Mairal, Priya Goyal, Piotr Bojanowski, and Armand Joulin. Unsupervised learning of visual features by contrasting cluster assignments. In *NeurIPS*, 2020. 1
- [10] Joao Carreira and Andrew Zisserman. Quo vadis, action recognition? a new model and the kinetics dataset. In *CVPR*, 2017. 7, 8
- [11] Brandon Castellano. Video scene cut detection and analysis tool. <https://github.com/Breakthrough/PySceneDetect>. 6
- [12] Shixing Chen, Xiaohan Nie, David Fan, Dongqing Zhang, Vimal Bhat, and Raffay Hamid. Shot contrastive self-supervised learning for scene boundary detection. In *CVPR*, 2021. 3
- [13] Ting Chen, Simon Kornblith, Mohammad Norouzi, and Geoffrey Hinton. A simple framework for contrastive learning of visual representations. In *ICML*, 2020. 1
- [14] Xinlei Chen, Haoqi Fan, Ross Girshick, and Kaiming He. Improved baselines with momentum contrastive learning. *arXiv preprint arXiv:2003.04297*, 2020. 6, 7
- [15] Madalena Costa, Ary L Goldberger, and C-K Peng. Multiscale entropy analysis of complex physiologic time series. *Physical review letters*, 2002. 1
- [16] Navneet Dalal and Bill Triggs. Histograms of oriented gradients for human detection. In *CVPR*, 2005. 5
- [17] Ali Diba, Vivek Sharma, Luc Van Gool, and Rainer Stiefelhagen. Dynamonet: Dynamic action and motion network. In *ICCV*, 2019. 7
- [18] Li Ding and Chenliang Xu. Weakly-supervised action segmentation with iterative soft boundary assignment. In *CVPR*, 2018. 3
- [19] Christoph Feichtenhofer, Haoqi Fan, Jitendra Malik, and Kaiming He. Slowfast networks for video recognition. In *ICCV*, 2019. 7
- [20] Christoph Feichtenhofer, Haoqi Fan, Bo Xiong, Ross Girshick, and Kaiming He. A large-scale study on unsupervised spatiotemporal representation learning. In *CVPR*, 2021. 1, 2, 3, 4, 6, 7
- [21] Pedro F Felzenszwalb, Ross B Girshick, David McAllester, and Deva Ramanan. Object detection with discriminatively trained part-based models. *TPAMI*, 2009. 5
- [22] Basura Fernando, Hakan Bilen, Efstratios Gavves, and Stephen Gould. Self-supervised video representation learning with odd-one-out networks. In *CVPR*, 2017. 3
- [23] Li Fu, Xiaoxiao Li, Runyu Wang, Zhengchen Zhang, Youzheng Wu, Xiaodong He, and Bowen Zhou. Scala: Supervised contrastive learning for end-to-end automatic speech recognition. *arXiv preprint arXiv:2110.04187*, 2021. 1
- [24] Chuang Gan, Boqing Gong, Kun Liu, Hao Su, and Leonidas J Guibas. Geometry guided convolutional neural networks for self-supervised video representation learning. In *CVPR*, 2018. 3
- [25] Rohit Girdhar, Joao Carreira, Carl Doersch, and Andrew Zisserman. Video action transformer network. In *CVPR*, 2019. 7
- [26] Ross Girshick, Jeff Donahue, Trevor Darrell, and Jitendra Malik. Rich feature hierarchies for accurate object detection and semantic segmentation. In *CVPR*, 2014. 5
- [27] Daniel Gordon, Kiana Ehsani, Dieter Fox, and Ali Farhadi. Watching the world go by: Representation learning from unlabeled videos. *arXiv preprint arXiv:2003.07990*, 2020. 6
- [28] Priya Goyal, Piotr Dollár, Ross Girshick, Pieter Noordhuis, Lukasz Wesolowski, Aapo Kyrola, Andrew Tulloch, Yangqing Jia, and Kaiming He. Accurate, large mini-batch sgd: Training imagenet in 1 hour. *arXiv preprint arXiv:1706.02677*, 2017. 5
- [29] Raghav Goyal, Samira Ebrahimi Kahou, Vincent Michalski, Joanna Materzynska, Susanne Westphal, Heuna Kim, Valentin Haenel, Ingo Fruend, Peter Yianilos, Moritz Mueller-Freitag, et al. The” something something” video database for learning and evaluating visual common sense. In *ICCV*, 2017. 6
- [30] Jean-Bastien Grill, Florian Strub, Florent Alché, Corentin Tallec, Pierre H Richemond, Elena Buchatskaya, Carl Doersch, Bernardo Avila Pires, Zhaohan Daniel Guo, Mohammad Gheshlaghi Azar, et al. Bootstrap your own latent: A new approach to self-supervised learning. In *NeurIPS*, 2020. 1
- [31] Tengda Han, Weidi Xie, and Andrew Zisserman. Video representation learning by dense predictive coding. In *ICCV Workshops*, 2019. 3, 7

- [32] Tengda Han, Weidi Xie, and Andrew Zisserman. Memory-augmented dense predictive coding for video representation learning. In *ECCV*, 2020. 3, 7
- [33] Tengda Han, Weidi Xie, and Andrew Zisserman. Self-supervised co-training for video representation learning. In *NeurIPS*, 2020. 3, 7
- [34] Kaiming He, Haoqi Fan, Yuxin Wu, Saining Xie, and Ross Girshick. Momentum contrast for unsupervised visual representation learning. In *CVPR*, 2020. 1
- [35] Tong He, Zhi Zhang, Hang Zhang, Zhongyue Zhang, Junyuan Xie, and Mu Li. Bag of tricks for image classification with convolutional neural networks. In *CVPR*, 2019. 5
- [36] Qingqiu Huang, Yu Xiong, Anyi Rao, Jiaze Wang, and Dahua Lin. Movienet: A holistic dataset for movie understanding. In *ECCV*, 2020. 3
- [37] Yu-Gang Jiang, Jingen Liu, Amir R. Zamir, George Toderici, Ivan Laptev, Mubarak Shah, and Rahul Sukthankar. Thumos challenge: Action recognition with a large number of classes. <http://crcv.ucf.edu/THUMOS14/>, 2014. 3, 6
- [38] Longlong Jing and Yingli Tian. Self-supervised spatiotemporal feature learning by video geometric transformations. *arXiv preprint arXiv:1811.11387*, 2018. 3, 7
- [39] Will Kay, Joao Carreira, Karen Simonyan, Brian Zhang, Chloe Hillier, Sudheendra Vijayanarasimhan, Fabio Viola, Tim Green, Trevor Back, Paul Natsev, et al. The kinetics human action video dataset. *arXiv preprint arXiv:1705.06950*, 2017. 1, 5, 6
- [40] Dahun Kim, Donghyeon Cho, and In So Kweon. Self-supervised video representation learning with space-time cubic puzzles. In *AAAI*, 2019. 3, 7
- [41] Bruno Korbar, Du Tran, and Lorenzo Torresani. Cooperative learning of audio and video models from self-supervised synchronization. In *NeurIPS*, 2018. 3
- [42] Hildegard Kuehne, Hueihan Jhuang, Estíbaliz Garrote, Tomaso Poggio, and Thomas Serre. Hmdb: a large video database for human motion recognition. In *ICCV*, 2011. 1, 6
- [43] Colin Lea, Austin Reiter, René Vidal, and Gregory D Hager. Segmental spatiotemporal cnns for fine-grained action segmentation. In *ECCV*, 2016. 3, 6
- [44] Hsin-Ying Lee, Jia-Bin Huang, Maneesh Singh, and Ming-Hsuan Yang. Unsupervised representation learning by sorting sequences. In *ICCV*, 2017. 3
- [45] Ang Li, Meghana Thotakuri, David A Ross, João Carreira, Alexander Vostrikov, and Andrew Zisserman. The ava-kinetics localized human actions video dataset. *arXiv preprint arXiv:2005.00214*, 2020. 3, 7
- [46] Rui Li, Yiheng Zhang, Zhaofan Qiu, Ting Yao, Dong Liu, and Tao Mei. Motion-focused contrastive learning of video representations. In *ICCV*, 2021. 6, 7
- [47] Yingwei Li, Yi Li, and Nuno Vasconcelos. Resound: Towards action recognition without representation bias. In *ECCV*, 2018. 6
- [48] Ji Lin, Chuang Gan, and Song Han. Tsm: Temporal shift module for efficient video understanding. In *ICCV*, 2019. 7
- [49] Tianwei Lin, Xiao Liu, Xin Li, Errui Ding, and Shilei Wen. Bmn: Boundary-matching network for temporal action proposal generation. In *ICCV*, 2019. 3, 6
- [50] Tianwei Lin, Xu Zhao, Haisheng Su, Chongjing Wang, and Ming Yang. Bsn: Boundary sensitive network for temporal action proposal generation. In *ECCV*, 2018. 3
- [51] Fuchen Long, Ting Yao, Zhaofan Qiu, Xinmei Tian, Jiebo Luo, and Tao Mei. Gaussian temporal awareness networks for action localization. In *CVPR*, 2019. 3
- [52] William Lotter, Gabriel Kreiman, and David Cox. Deep predictive coding networks for video prediction and unsupervised learning. *arXiv preprint arXiv:1605.08104*, 2016. 3
- [53] Antoine Miech, Jean-Baptiste Alayrac, Lucas Smaira, Ivan Laptev, Josef Sivic, and Andrew Zisserman. End-to-end learning of visual representations from uncurated instructional videos. In *CVPR*, 2020. 3
- [54] Alejandro Pardo, Fabian Caba, Juan León Alcázar, Ali K Thabet, and Bernard Ghanem. Learning to cut by watching movies. In *ICCV*, 2021. 3
- [55] Mandela Patrick, Yuki M Asano, Ruth Fong, João F Henriques, Geoffrey Zweig, and Andrea Vedaldi. Multi-modal self-supervision from generalized data transformations. *arXiv preprint arXiv:2003.04298*, 2020. 3
- [56] AJ Piergiovanni, Anelia Angelova, and Michael S. Ryoo. Evolving losses for unsupervised video representation learning. In *CVPR*, 2020. 3
- [57] Rui Qian, Tianjian Meng, Boqing Gong, Ming-Hsuan Yang, Huisheng Wang, Serge Belongie, and Yin Cui. Spatiotemporal contrastive video representation learning. In *CVPR*, 2021. 1, 2, 3, 4, 5, 6, 7, 8, 12
- [58] Adrià Recasens, Pauline Luc, Jean-Baptiste Alayrac, Luyu Wang, Florian Strub, Corentin Tallec, Mateusz Malinowski, Viorica Patraucean, Florent Althé, Michal Valko, et al. Broaden your views for self-supervised video learning. In *ICCV*, 2021. 1, 2, 3, 4
- [59] Shaoqing Ren, Kaiming He, Ross Girshick, and Jian Sun. Faster r-cnn: Towards real-time object detection with region proposal networks. In *NeurIPS*, 2015. 5
- [60] Alexander Richard, Hilde Kuehne, and Juergen Gall. Weakly supervised action learning with rnn based fine-to-coarse modeling. In *CVPR*, 2017. 3
- [61] Arka Sadhu, Tanmay Gupta, Mark Yatskar, Ram Nevatia, and Aniruddha Kembhavi. Visual semantic role labeling for video understanding. In *CVPR*, 2021. 1, 2, 3, 4, 5, 12
- [62] Dian Shao, Yue Zhao, Bo Dai, and Dahua Lin. Finegym: A hierarchical video dataset for fine-grained action understanding. In *CVPR*, 2020. 3
- [63] Dian Shao, Yue Zhao, Bo Dai, and Dahua Lin. Intra-and inter-action understanding via temporal action parsing. In *CVPR*, 2020. 3
- [64] Mike Zheng Shou, Stan Lei, Deepti Ghadiyaram, Weiyao Wang, and Matt Feiszli. Generic event boundary detection: A benchmark for event segmentation. <https://github.com/StanLei52/GEED/tree/main/eval>, 2021. 12
- [65] Mike Zheng Shou, Stan W Lei, Weiyao Wang, Deepti Ghadiyaram, and Matt Feiszli. Generic event boundary detection: A benchmark for event segmentation. In *ICCV*, 2021. 1, 2, 3, 4, 5, 6, 12
- [66] Zheng Shou, Jonathan Chan, Alireza Zareian, Kazuyuki Miyazawa, and Shih-Fu Chang. Cdc: Convolutional-de-

- convolutional networks for precise temporal action localization in untrimmed videos. In *CVPR*, 2017. 3
- [67] Zheng Shou, Dongang Wang, and Shih-Fu Chang. Temporal action localization in untrimmed videos via multi-stage cnns. In *CVPR*, 2016. 3
- [68] Panagiotis Sidiropoulos, Vasileios Mezaris, Ioannis Kompatsiaris, Hugo Meinedo, Miguel Bugalho, and Isabel Trancoso. Temporal video segmentation to scenes using high-level audiovisual features. *TCSVT*, 2011. 3, 4
- [69] Ankit Singh, Omprakash Chakraborty, Ashutosh Varshney, Rameswar Panda, Rogerio Feris, Kate Saenko, and Abir Das. Semi-supervised action recognition with temporal contrastive learning. In *CVPR*, 2021. 3
- [70] Khurram Soomro, Amir Roshan Zamir, and Mubarak Shah. Ucf101: A dataset of 101 human actions classes from videos in the wild. *arXiv preprint arXiv:1212.0402*, 2012. 1, 6
- [71] Nitish Srivastava, Elman Mansimov, and Ruslan Salakhudinov. Unsupervised learning of video representations using lstms. In *ICML*, 2015. 3
- [72] Chen Sun, Fabien Baradel, Kevin Murphy, and Cordelia Schmid. Learning video representations using contrastive bidirectional transformer. *arXiv preprint arXiv:1906.05743*, 2019. 3
- [73] Chen Sun, Austin Myers, Carl Vondrick, Kevin Murphy, and Cordelia Schmid. Videobert: A joint model for video and language representation learning. In *ICCV*, 2019. 3
- [74] Barbara Tversky and Jeffrey M Zacks. Event perception. *Oxford handbook of cognitive psychology*, 2013. 3
- [75] Jue Wang, Gedas Bertasius, Du Tran, and Lorenzo Torresani. Long-short temporal contrastive learning of video transformers. *arXiv preprint arXiv:2106.09212*, 2021. 3, 4
- [76] Jiangliu Wang, Jianbo Jiao, Linchao Bao, Shengfeng He, Yunhui Liu, and Wei Liu. Self-supervised spatio-temporal representation learning for videos by predicting motion and appearance statistics. In *CVPR*, 2019. 3, 7
- [77] Jiangliu Wang, Jianbo Jiao, and Yun-Hui Liu. Self-supervised video representation learning by pace prediction. In *ECCV*, 2020. 3, 7
- [78] Limin Wang, Yuanjun Xiong, Zhe Wang, Yu Qiao, Dahua Lin, Xiaoou Tang, and Luc Van Gool. Temporal segment networks: Towards good practices for deep action recognition. In *ECCV*, 2016. 7
- [79] Dejing Xu, Jun Xiao, Zhou Zhao, Jian Shao, Di Xie, and Yueting Zhuang. Self-supervised spatiotemporal learning via video clip order prediction. In *CVPR*, 2019. 3, 7
- [80] Jiarui Xu and Xiaolong Wang. Rethinking self-supervised correspondence learning: A video frame-level similarity perspective. In *ICCV*, 2021. 7, 8
- [81] Ceyuan Yang, Yinghao Xu, Bo Dai, and Bolei Zhou. Video representation learning with visual tempo consistency. *arXiv preprint arXiv:2006.15489*, 2020. 6
- [82] Ting Yao, Yiheng Zhang, Zhaofan Qiu, Yingwei Pan, and Tao Mei. Seco: Exploring sequence supervision for unsupervised representation learning. In *AAAI*, 2021. 6, 7
- [83] Hang Zhao, Antonio Torralba, Lorenzo Torresani, and Zhicheng Yan. Hacs: Human action clips and segments dataset for recognition and temporal localization. In *ICCV*, 2019. 3
- [84] Yue Zhao, Yuanjun Xiong, Limin Wang, Zhirong Wu, Xiaoou Tang, and Dahua Lin. Temporal action detection with structured segment networks. In *ICCV*, 2017. 3
- [85] Xingyi Zhou, Dequan Wang, and Philipp Krähenbühl. Objects as points. *arXiv preprint arXiv:1904.07850*, 2019. 7

A. Additional Implementation Details

A.1. VidSitu

VidSitu [61] contains 23.6k training, 1.3k validation and 1.3k test videos. Since the test set is held out for a challenge, we benchmark on the validation set. We download the videos with 720×1280 resolution and 30 frame-per-second, using the script provided by the authors. During training, we apply random cropping with the area ratio set as (0.3, 1.0) and then resize frames to 224×224 as in [57].

A.2. Kinetics-GEBD

Kinetics-GEBD [65] annotates 20k out of 240k training videos and all 20k validation videos from Kinetics-400. Each video is annotated by 5 sets of event boundaries. The multi-labeling does not affect our self-supervised pre-training stage since no labels are used.

For generating training clips, we adopt the practice from the dataset authors by selecting the annotation entry with the highest F1 consistency score with other entries. The annotation is in the format of timestamps and we choose the closest frame to a ground truth timestamp as an event boundary. We adopt a 32-frame long sliding window with a stride of 3-frame. The 16th frame of the sliding window is considered as the center frame, and the window would get a positive label when the time difference between the center frame and ground truth is less than 0.15 second.

During fine-tuning, we sample a clip of 16 frames with a stride of 2 inside each window, and feed it into the video encoder. No temporal augmentation is applied. Instead of global average pooling, we conduct two separate average pooling before and after the center frame. We then concatenate the two features and perform binary classification.

For prediction, we use the same sliding window and stride as in training. If a window is classified as positive, we use the timestamp of the center frame as the detected boundary. We would merge consecutive positive predictions into a single prediction by averaging their predicted timestamps.

Please refer to the original paper [65] and the challenge evaluation code [64] for details on how to deal with multiple ground truths and calculate the final F1 score.

B. Visualization of Feature Similarity

We provide a visualization of feature similarity to demonstrate the difference between temporally persistent and fine-grained features. Concretely, for every video in VidSitu validation set, we uniformly sample 5 consecutive clips and feed them into the trained video encoder to get their feature vectors. We then calculate the cosine similarities between all pairs of features, forming a 5×5 similarity matrix. We extract learned features from two video encoders **TeG-PS** and **TeG-FG** introduced in Section 5.1.

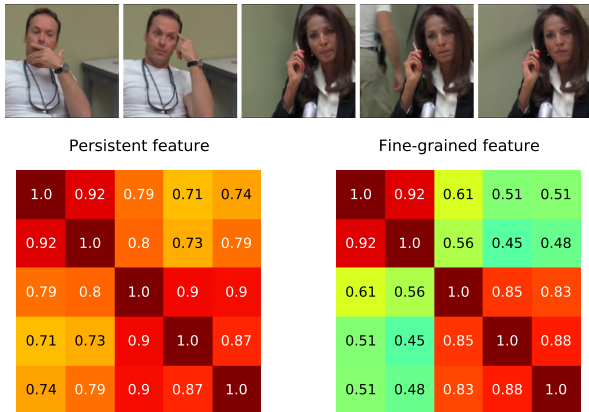


Figure 5. **Visualization of feature similarity.** Top row shows the center frame of each input clip. The left matrix is the similarity matrix of temporally persistent features and the right one comes from temporally fine-grained features.

Figure 5 shows a representative example. Take the first row of the similarity matrix as an example, the 5 entries in the first row represent the feature similarity between (clip 1, clip 1), (clip 1, clip 2), ..., (clip 1, clip 5). Despite the great difference between two groups of clip 1-2 and clip 3-5, the temporally persistent features still obtain cosine similarities larger than 0.7. While for temporally fine-grained features, the similarities drop to around 0.45-0.6. This example clearly shows that temporally fine-grained features are more sensitive to the temporal content changes compared with temporally persistent features.

Additional randomly selected examples are shown in Figure 6. From these examples, we can see that temporally persistent features would generally produce higher similarity scores compared with temporally fine-grained features. We also draw a further observation that temporally fine-grained features are robust when the temporal content within the video changes very little (see the example in row 5, column 1 of Figure 6).

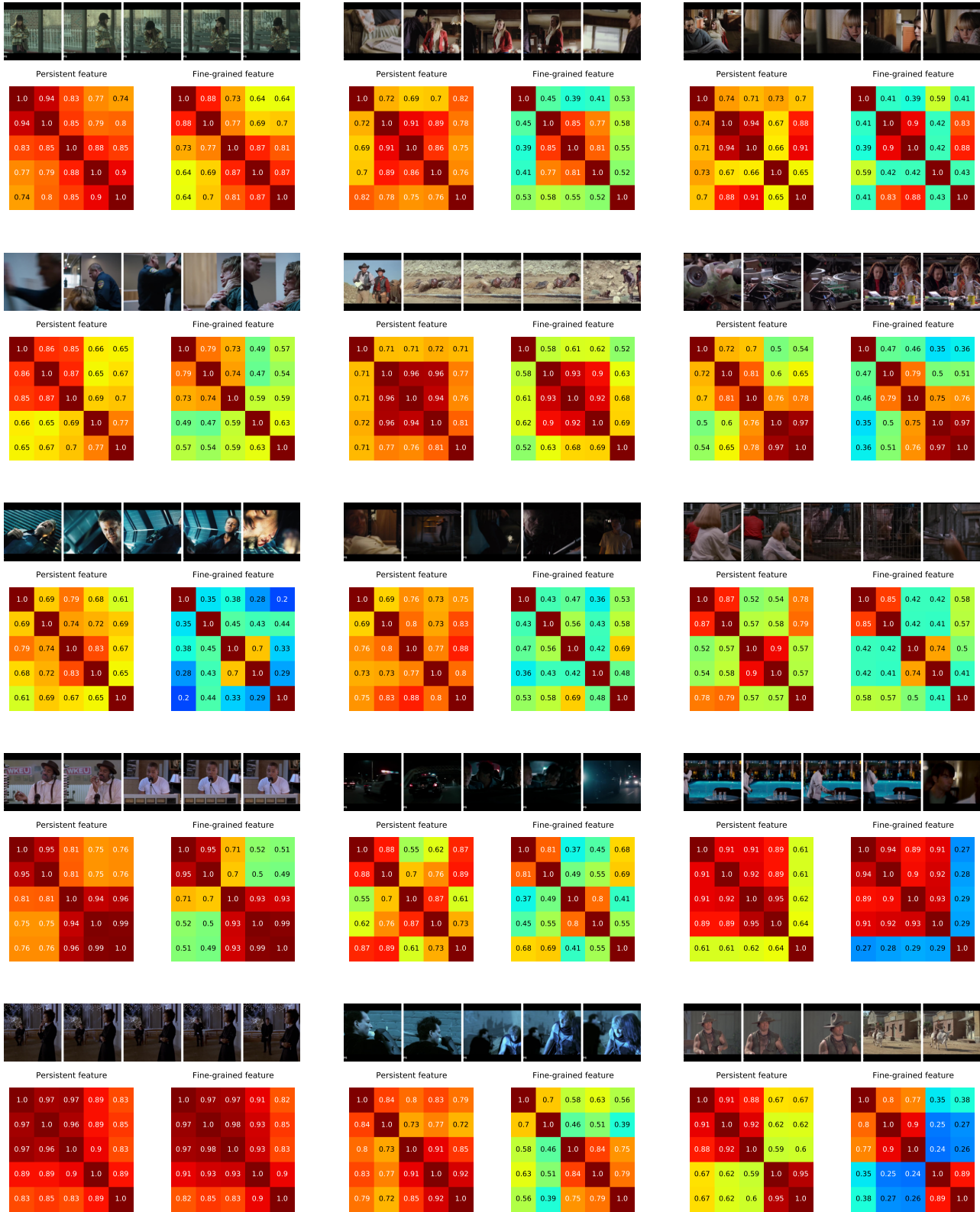


Figure 6. **Random examples** of feature similarity on VidSitu validation videos. In each subfigure, we show the input video (top), the similarity matrices of temporally persistent features (bottom left) and temporally fine-grained features (bottom right).